Insect Biochemistry and Molecular Biology 43 (2013) 219–228

Contents lists available at SciVerse ScienceDirect

Insect Biochemistry and Molecular Biology

journal homepage: www.elsevier.com/locate/ibmb

Cloning and characterization of a microsomal epoxide hydrolase from *Heliothis virescens*

Shizuo G. Kamita, Kohji Yamamoto [1], Mary M. Dadala [2], Khavong Pha [3], Christophe Morisseau, Aurélie Escaich, Bruce D. Hammock*

Department of Entomology and UC Davis Comprehensive Cancer Center, University of California, Davis, CA 95616, USA

ARTICLE INFO

Article history:
Received 15 November 2012
Received in revised form
7 December 2012
Accepted 10 December 2012

Keywords:
Epoxide hydrolase
Heliothis virescens
Fluorescent substrate
Inhibitor
Xenobiotic

ABSTRACT

Epoxide hydrolases (EHs) are α/β-hydrolase fold superfamily enzymes that convert epoxides to 1,2-*trans* diols. In insects EHs play critical roles in the metabolism of toxic compounds and allelochemicals found in the diet and for the regulation of endogenous juvenile hormones (JHs). In this study we obtained a full-length cDNA, *hvmeh1*, from the generalist feeder *Heliothis virescens* that encoded a highly active EH, Hv-mEH1. Of the 10 different EH substrates that were tested, Hv-mEH1 showed the highest specific activity (1180 nmol min^{-1} mg^{-1}) for a 1,2-disubstituted epoxide-containing fluorescent substrate. This specific activity was more than 25- and 3900-fold higher than that for the general EH substrates *cis*-stilbene oxide and *trans*-stilbene oxide, respectively. Although phylogenetic analysis placed Hv-mEH1 in a clade with some lepidopteran JH metabolizing EHs (JHEHs), JH III was a relatively poor substrate for Hv-mEH1. Hv-mEH1 showed a unique substrate selectivity profile for the substrates tested in comparison to those of MsJHEH, a well-characterized JHEH from *Manduca sexta*, and hmEH, a human microsomal EH. Hv-mEH1 also showed unique enzyme inhibition profiles to JH-like urea, JH-like secondary amide, JH-like primary amide, and non-JH-like primary amide compounds in comparison to MsJHEH and hmEH. Although Hv-mEH1 is capable of metabolizing JH III, our findings suggest that this enzymatic activity does not play a significant role in the metabolism of JH in the caterpillar. The ability of Hv-mEH1 to rapidly hydrolyze 1,2-disubstituted epoxides suggests that it may play roles in the metabolism of fatty acid epoxides such as those that are commonly found in the diet of *Heliothis*.

1. Introduction

Heliothinae is a subfamily of about 400 noctuid moth species that are found in temperate and tropical regions throughout the world (Mitter et al., 1993). Many species in this subfamily show behavioral, physiological, and ecological characteristics such as polyphagy, high mobility, facultative diapause, and high fecundity that make them exceptional agricultural pests (Fitt, 1989). Heliothine caterpillars in the genus *Heliothis* and related genus *Helicoverpa* are major pests that feed on high value, low damage threshold agricultural crops (e.g., cotton, tobacco, sweet corn, and tomato) and horticultural plantings. In the United States, heliothine caterpillars such as the tobacco budworm *Heliothis virescens* are estimated to cause over $1 billion in annual economic losses both in terms of direct crop reductions and indirectly in terms of costs associated with their control (Fitt, 1989). The highly polyphagous behavior of *H. virescens* and other heliothine caterpillars suggests that they will ingest and come into contact with a wide variety of epoxide containing compounds (e.g., plant allelochemicals,

Abbreviations: EH, epoxide hydrolase; JH, juvenile hormone; JHEH, JH epoxide hydrolase; hvmeh1, full-length EH-encoding cDNA from *Heliothis virescens*; Hv-mEH1, microsomal EH from *H. virescens*; *c*-SO, *cis*-stilbene oxide; *t*-SO, *trans*-stilbene oxide; *t*-DPPO, *trans*-diphenylpropene oxide; *Bommo*-JHEH and BmJHEH, JHEH from *Bombyx mori*; MsJHEH, JHEH from *Manduca sexta*; hmEH, human microsomal EH; TmEH1, microsomal EH from *Trichoplusia ni*; TcJHEH-r3, JHEH from *Tribolium castaneum*; MNHE, cyano(2-methoxynaphthalen-6-yl)methyl *trans*-2-(3-propyloxiran-2-yl)acetate; MNPE, cyano(2-methoxynaphthalen-6-yl)methyl *trans*-(2-(3-phenyloxiran-2-yl))acetate; MNPEC, cyano-(6-methoxy-naphthalen-2-yl)-methyl *trans*-((3-ethyl-oxiran-2-yl)methyl) carbonate; MNiPC, cyano-(6-methoxy-naphthalen-2-yl)-methyl 3,3-dimethyl-oxiranylmethyl carbonate; MNPC, cyano(6-methoxy-naphthalen-2-yl)methyl *trans*-[(3-phenyloxiran-2-yl)methyl] carbonate; CMNGC, cyano(6-methoxy-naphthalen-2-yl)methyl oxiran-2-ylmethyl carbonate; OTFP, 3-octylthio-1,1,1-trifluoropropan-2-one.

* Corresponding author. Tel.: +1 530 752 7519; fax: +1 530 752 1537.
E-mail address: bdhammock@ucdavis.edu (B.D. Hammock).
[1] Present address: Faculty of Agriculture, Kyushu University, Fukuoka, Japan.
[2] Present address: Department of Sericulture, Sri Padmavati Women's University, Tirupati, Andhra Pradesh, India.
[3] Present address: Department of Microbiology, University of California, Davis, CA, USA.

0965-1748/$ – see front matter © 2012 Elsevier Ltd. All rights reserved.
http://dx.doi.org/10.1016/j.ibmb.2012.12.002

antifeedants, and hormones/hormone precursors) (see Mullin, 1988). The ability to detoxify or metabolize these epoxides is likely to be an important factor in the success of these caterpillars.

Epoxide hydrolases (EHs) are α/β-hydrolase fold superfamily enzymes that convert epoxides to 1,2-diols. In insects, microsomal EHs (EC 3.3.2.9) are known to metabolize epoxide containing xenobiotics, allelochemicals, and antifeedants that are commonly encountered in the diet of polyphagous insects (reviewed in Mullin, 1988; Morisseau and Hammock, 2008). Microsomal EHs are also known to help reduce the titer of juvenile hormones (JHs), hormones that regulate metamorphosis, behavior, development, reproduction, and other key biological events in insects (reviewed in Goodman and Granger, 2005; Riddiford, 2008). Seven forms of JH (JH 0, JH I, JH II, JH III, 4-methyl JH I, JH III bisepoxide, and JH III skipped bisepoxide) have been identified in insects (Goodman and Granger, 2005; Kotaki et al., 2009). Structurally, JHs are sesquiterpenes with an epoxide at one end or near the end of the molecule and at the other end an α,β-unsaturated methyl ester (Fig. 1). The epoxide of JH is metabolized by a JH epoxide hydrolase (JHEH) (reviewed in Goodman and Granger, 2005) and the methyl ester by a JH-selective esterase (reviewed in Kamita and Hammock, 2010).

Structurally, the substrate-binding pocket of EH is composed of core and lid domains. The core domain contains the catalytic triad composed of a catalytic nucleophile (aspartic acid), water activating basic amino acid residue (histidine), and acidic residue (aspartic or glutamic acid) (reviewed in Morisseau and Hammock, 2008; Decker et al., 2009). The lid domain contains two tyrosine residues that help to position the epoxide within the substrate binding pocket. An oxyanion hole motif composed of the conserved HGXP motif (where X is usually an aromatic amino acid residue) is also conserved in EH. The proposed reaction that is catalyzed by EH has two major steps (reviewed in Morisseau and Hammock, 2005). In the first step, tyrosine residues that are found in the lid domain polarize the epoxide. Simultaneously, the carboxylic acid of the aspartic acid residue (found on the opposite side of the binding pocket as the tyrosine residues) makes a "backside" attack of one of the epoxide carbons (usually the least sterically hindered and/or most reactive) leading to *trans* hydration of the epoxide. The histidine residue and second acidic residue form a proton shuttle that helps to activate and orient the carboxylic acid of the aspartic acid residue. Opening of the epoxide results in the formation of a complex called the hydroxyl-alkyl-enzyme intermediate in which an ester (between the substrate and carboxylic acid of the enzyme and substrate) and alcohol are formed. Urea and amide compounds that mimic this transition state intermediate have been designed as potent inhibitors of EH. In the second step, the histidine-second acidic amino acid residue combination activates a water molecule which now attacks the carbonyl of the ester (the intermediate state in this case is stabilized by the oxyanion hole) resulting in a second alcohol (i.e., formation of the diol) and regeneration of the original aspartic acid residue.

A wide range of epoxide-containing substrates are available for characterizing the enzyme kinetics of EHs. Radiolabeled substrates (Table 1) such as *cis*-stilbene oxide (*c*-SO), *trans*-stilbene oxide (*t*-SO), and *trans*-diphenylpropene oxide (*t*-DPPO) (Gill et al., 1983; Borhan et al., 1995) are commonly used with microsomal and soluble (i.e., soluble following ultracentrifugation at greater than 100,000 × g) EH. Spectrophotometric substrates such as 4-nitro-

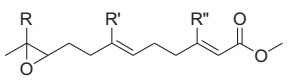

JH III: R = R' = R" = CH_3
JH II: R = CH_2CH_3, R' = R" = CH_3
JH I: R = R' = CH_2CH_3, R" = CH_3
JH 0: R = R' = R" = CH_2CH_3

Fig. 1. Structure of juvenile hormone (JH) III, JH II, JH I, and JH 0. At least seven forms of JH have been isolated from insects. All of the JHs that have been identified to date have an epoxide and a methyl ester.

Table 1
Hydrolysis of general epoxide substrates and JH III by Hv-mEH1 and MsJHEH.

Substrate	Structure	Specific activity[a] (nmol min^{-1} mg^{-1})	
		Hv-mEH1	MsJHEH
c-SO	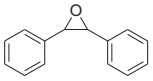	45.8 ± 7.0	3.7 ± 0.5
t-SO	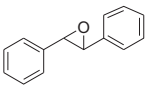	0.3 ± 0.01	2.1 ± 0.3
t-DPPO	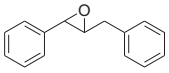	0.1 ± 0.04	18.3 ± 4.0
JH III[b]	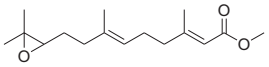	1.7 ± 0.1	59

[a] The enzyme assays were performed in 100 mM sodium phosphate, pH 8.0, containing 50 μM substrate (5 μM for JH III), 1% (v:v) ethanol, and 0.1 mg ml^{-1} BSA at 30 °C. The values were corrected for background hydrolysis. The results shown are the mean ± standard deviation of at least three separate experiments.
[b] V_{max} values are shown for JH III. The V_{max} value for MsJHEH is from Severson et al. (2002).

phenyl-*trans*-2,3-epoxy-3-phenylpropyl carbonate (NEPC) (Dietze et al., 1994) and fluorescent substrates (Jones et al., 2005; Morisseau et al., 2011) have also been developed for characterizing EH activity and for screening the selectivity and potency of compounds that inhibit microsomal and soluble EH. Fluorescent substrates that have been developed in our laboratory show up to two orders of magnitude of improved sensitivity in comparison to spectrophotometric EH substrates (Jones et al., 2005; Morisseau et al., 2011). The mode of action of these fluorescent substrates is based on a fluorescent, aromatic aldehyde reporter that is formed following the intramolecular cyclization of the diol that is formed following hydrolysis of epoxide containing α-cyanoesters (Shan and Hammock, 2001; Wheelock et al., 2003; Jones et al., 2005).

In this study we obtained a full-length epoxide hydrolase-encoding cDNA, *hvmeh1*, from the tobacco budworm *H. virescens*. The recombinant protein, Hv-mEH1, encoded by *hvmeh1* showed high amino acid sequence identity to JHEHs from the lepidopterans *Bombyx mori* (*Bommo*-JHEH (Zhang et al., 2005)) and *Manduca sexta* (MsJHEH (Wojtasek and Prestwich, 1996)). This high identity suggested that Hv-mEH1 encoded a biologically active JHEH. Hv-mEH1, however, metabolized JH III with significantly slower V_{max}, higher K_M, and slower turnover values in comparison to *Bommo*-JHEH and MsJHEH. Hv-mEH1 showed a specific activity for *c*-SO that was about 10-fold higher than that of MsJHEH. Of 10 different epoxide containing substrates that were tested with Hv-mEH1, Hv-mEH1 showed the highest activity for a fluorescent substrate containing an aliphatic 1,2-disubstituted epoxide. Of 33 urea and amide compounds that were tested, primary amides showed the highest inhibitory potency with Hv-mEH1. Taken together our findings suggested that JH III is not a major endogenous substrate for Hv-mEH1. Instead, Hv-mEH1 may play roles in the hydrolysis of yet unknown endogenous substrates or in the metabolism of a diverse range of epoxides (reviewed in Mullin, 1988) that are found in the diet of this polyphagous insect.

2. Materials and methods

2.1. Insects and insect rearing

Eggs of the tobacco budworm *H. virescens* were obtained from Benzon Research. Larval *H. virescens* were reared on ready-to-use

hornworm diet (Carolina Biological Supply) under a 12 h light:12 h dark cycle at 27 °C, 60% relative humidity.

2.2. Cloning of a full-length EH-encoding cDNA, hvmeh1, from larval H. virescens

Total RNA was isolated from fat body tissues collected from 5th instar larvae (day 1 post ecdysis) of *H. virescens*. The fat body tissues from 15 larvae were collected into 1 ml of RNA*later* (Ambion), and 50 μl of this suspension was used for total RNA isolation with TRIzol LS Reagent (Invitrogen) following manufacturer's protocol. Four micrograms of the total RNA was used to generate double-stranded cDNAs using a Creator SMART cDNA Library Construction kit (Clontech) following the manufacturer's protocol. The double-stranded cDNAs were used as template for 3′- and 5′-RACE procedures to identify the 3′- and 5′-end sequences of a cDNA, *hvmeh1*, encoding a potential EH.

The 3′-end and 3′-UTR of *hvmeh1* were amplified by PCR using the degenerate primer JHEH6for (5′-GC(C/T)AC(G/C)AA(A/G) CCTGA(C/T)AC(A/T)(A/G)TTGG-3′) and anchor primer CDSIIIshort (5′-ATTCTAGAGGCCGAGGCGGCCGAC-3′). The JHEH6for primer was designed on the basis of a sequence of amino acid residues, ATKPDT(I/V)G, that is highly conserved in known lepidopteran and non-lepidopteran JHEHs. A touchdown PCR amplification was performed with these primers using Advantage HF 2 polymerase (Clontech) as follows: 94 °C, 2 min; 20 cycles of 94 °C, 15 s; 55 °C–45 °C (−0.5 °C per cycle), 30 s; and 68 °C, 30 s; followed immediately by 19 cycles of 94 °C, 15 s; 50 °C, 30 s; 68 °C, 30 s; and a final cycle of 68 °C, 2 min. This PCR generated a 0.5 kbp-long amplicon that was column-purified (Qiagen), inserted into the pCR-Blunt II-TOPO cloning vector (Invitrogen), and the resulting circular DNA was transformed into One Shot TOP10 chemically competent *E. coli* (Invitrogen) following the manufacturer's protocol. The sequence of the insert was determined by the UC Davis College of Biological Sciences Sequencing Facility. The deduced amino acid sequence of the insert was consistent with the C-terminal of a potential EH.

The 5′-UTR and 5′-end of *hvmeh1* were amplified by PCR using the anchor primer SMARTshort (5′-AGAGTGGCCATTACGGCCGGG-3′), and gene-specific primer HvGSP3 (5′-GAGGCTGGTAGAA-TAGCTCTTCTTTCGC-3′). The PCR amplification was performed with Advantage HF 2 polymerase as follows: 94 °C, 2 min and 35 cycles of 94 °C, 15 s; 68 °C, 30 s; 68 °C, 2 min; and a final cycle of 68 °C, 5 min. The resulting 1.2 kbp-long amplicon was column-purified, ligated into pCR-Blunt II-TOPO, and the resulting circular DNA was transformed into One Shot TOP10 chemically competent *E. coli* as described above. The insert was sequenced as described above and the deduced amino acid sequence of the insert was found to encode the N-terminal of a potential EH.

After the 5′- and 3′-ends of *hvmeh1* were determined, the predicted EH-encoding open reading frame was amplified by PCR using the primers HvEH5Bgl (5′-GAAGATCTATGGGATTCCTTGTAAAAGCG-3′) and HvEH3Eco (5′-CGGAATTCTCACAGTTCAGTTTTCTTATTCTT-3′) and double-stranded cDNAs from *H. virescens* (see above) as template. These primers placed *Bgl*II and *Eco*RI restriction sites (underlined) at the 5′ and 3′ ends of the coding sequence, respectively. PCR amplification was performed using Advantage HF 2 polymerase as follows: 94 °C, 2 min; 5 cycles of 94 °C, 30 s; 58 °C, 30 s; and 68 °C, 30 s; 25 cycles of 94 °C, 30 s; 65 °C, 30 s; 68 °C, 2 min; and a final cycle of 68 °C, 5 min. The resulting 1.4 kbp-long amplicon was column-purified, ligated into pCR-Blunt II-TOPO, and transformed into One Shot TOP10 chemically competent *E. coli* as described above. The insert was then excised from the plasmid by digestion with *Bgl*II and *Eco*RI, gel-purified, ligated into the *Bgl*II and *Eco*RI cloning sites of the baculovirus transfer vector pAcUW21 (Weyer et al., 1990) using T4 DNA ligase (New England Biolabs). The ligation mixture was transformed into DH5α competent cells (Invitrogen) in order to generate the recombinant transfer vector pAcUW21-hvmeh1. The complete sequence of the putative EH-encoding coding sequence in pAcUW21-hvmeh1 was determined in both directions using pAcUW21- and hvmeh1-specific primers.

2.3. Protein expression and isolation of microsomes

A recombinant baculovirus expression vector, AcHvmEH1, was generated in Sf9 cells (Invitrogen) that were transfected with 2 μg of pAcUW21-hvmeh1 and 2 μg of *Bsu*36I-digested BacPAK6 baculovirus DNA (Clontech) using Cellfectin Transfection Reagent (Invitrogen) following the manufacturer's protocol. AcHvmEH1 was isolated from the supernatant of the transfected Sf9 cells by three rounds of plaque purification on Sf9 cells following standard procedures (Merrington et al., 1999). The Sf9 cells were cultured on ExCell 420 medium (SAFC Biosciences) supplemented with 2.5% fetal bovine serum at 27 °C. Recombinant baculoviruses AcMsJHEH (also known as SDCM1 (Debernard et al., 1998)) and AcEPHX1 (Yamada et al., 2000) that express recombinant MsJHEH and human microsomal EH (hmEH, also known as EPHX1), respectively, were previously described.

The recombinant proteins (Hv-mEH1, MsJHEH, and hmEH) were expressed in High Five cells (Invitrogen) that were inoculated with AcHvmEH1, AcMsJHEH or AcEPHX1 at a multiplicity of infection of 0.5 and cultured on ESF921 medium (Expression Systems) at 27 °C. The cells were generally harvested at 65 h postinfection (p.i.) by low speed centrifugation (230 × g, 15 min, 5 °C) and resuspended in homogenization buffer (50 mM Tris–HCl, pH 8.0, containing 1 mM phenylmethylsulfonyl fluoride (PMSF), 1 mM ethylenediaminetetraacetic acid (EDTA), and 1 mM dithiothreitol). The cells were homogenized on ice by three 15 s-long, 21,500 rpm, bursts of a Turrax T25 homogenizer (IKA-Werke), and the homogenate was subject to ultracentrifugation (163,000 × g, 60 min, 5 °C). The pellet from this centrifugation was resuspended in homogenization buffer containing 0.5% (v:v) Triton X-100 (100 mg wet weight of cells per ml of homogenization buffer) and homogenized on ice as described above by three 5 s-long bursts. The homogenate was then centrifuged again at 163,000 × g (60 min, 5 °C). The supernatant from this centrifugation was flash frozen in liquid nitrogen and stored at −80 °C.

The microsomal preparations were analyzed by sodium dodecyl sulfate-polyacrylamide gel electrophoresis (SDS-PAGE) using 4–12% Tris-glycine gels (Invitrogen) in Tris-glycine running buffer (Invitrogen). The gels were stained with Bio-Safe Coomassie stain (Bio-Rad) following the manufacturer's protocol. Following staining, the gels were analyzed using the ImageJ program (Rasband, 2006) to estimate the efficiency of the isolation protocol. Protein concentrations were determined using Bradford (Bio-Rad) or BCA (Pierce) protein assay reagents and bovine serum albumin fraction V (Sigma) to generate a standard curve.

2.4. Enzyme assays and kinetic constant determinations

2.4.1. Enzyme assays using radiolabeled substrates

The specific activity of Hv-mEH1 and MsJHEH for general epoxide substrates (i.e., *c*-SO, *t*-SO, and *t*-DPPO (Gill et al., 1983; Borhan et al., 1995)); and for JH III (PerkinElmer and Sigma–Aldrich) was determined by partition assays as previously described (Wixtrom and Hammock, 1985; Borhan et al., 1995; Hammock and Sparks, 1977). The partition assay with tritium-labeled *c*-SO, *t*-SO, and *t*-DPPO was routinely performed in 100 μl of 100 mM sodium phosphate buffer, pH 8.0, containing enzyme (Hv-mEH1 or MsJHEH), 50 μM substrate, 1% (v/v) ethanol, and 0.1 mg ml^{-1} of bovine serum albumin (BSA) at

30 °C so that no more than 15% of the substrate was hydrolyzed during the incubation period. The partition assay with tritium-labeled JH III was performed under the same conditions except that 5 μM substrate was used. In order to determine the effect of buffer pH on the activity of Hv-mEH1, the partition assay with JH III was performed using citrate-phosphate (pH 4.0 and 5.0), sodium phosphate (pH 6.0, 7.0, and 8.0) or glycine-sodium hydroxide (pH 9.0 and 10.0) buffer. Non-enzymatic hydrolysis of JH III was determined at each pH and subtracted as background. All of the assays were performed in triplicate and repeated at least three times.

The Michaelis constant (K_M) and V_{max} of Hv-mEH1 for JH III were determined using specific activity values that were obtained with eight different concentrations of JH III (96–11,190 nM) that bracketed the estimated K_M value using the SigmaPlot Enzyme Kinetics Module 1.1 software (Systat Software). The k_{cat} of Hv-mEH1 was calculated using an estimated molecular mass of 53.1 kDa. The assays were performed in triplicate and repeated three times. The enzyme concentration and/or assay time (5–30 min) were adjusted in these assays so that no more than 15% of the JH III substrate was hydrolyzed. The potential hydrolysis of the ester of JH III by contaminating esterases in the microsomal preparation was addressed by a 10 min-long preincubation at 30 °C with 10 μM 3-octylthio-1,1,1-trifluoropropan-2-one (OTFP), a highly potent esterase inhibitor (Abdel-Aal and Hammock, 1985).

```
        gagcattcagagctcactgccaccgcgtttgagctacacaccgacttacgacg
atgggattccttgtaaaagcggtgctggttgccgccctgggcgtgacggcatggtttgtc
 M  G  F  L  V  K  A  V  L  V  A  A  L  G  V  T  A  W  F  V    20
ctcaagtgctcgaaacctcacaccatcccccacttcgatagcgaagagtggtggggacca
 L  K  C  S  K  P  H  T  I  P  H  F  D  S  E  E  W  W  G  P    40
aaagagctgaaagaaactaaacaagaccagagcatcaggccgttcaagatcaaattcgac
 K  E  L  K  E  T  K  Q  D  Q  S  I  R  P  F  K  I  K  F  D    60
gaggaaatgataaaagacctaaaataccgcttaaagaaccatcgtaagttcacgccgcct
 E  E  M  I  K  D  L  K  Y  R  L  K  N  H  R  K  F  T  P  P    80
ctagaaggagttgcctttgagtatgggttcaatactgctcaactggactcctggctgacc
 L  E  G  V  A  F  E  Y  G  F  N  T  A  Q  L  D  S  W  L  T   100
tactgggctgataagtacaacttcagcgaacgcgaggctttcctcaacaagttccctcac
 Y  W  A  D  K  Y  N  F  S  E  R  E  A  F  L  N  K  F  P  H   120
ttcaaaactaagatccaaggcttggatgtacattttatcagggttaagccacaggtcccc
 F  K  T  K  I  Q  G  L  D  V  H  F  I  R  V  K  P  Q  V  P   140
aaagatgtggaagtaatcccgctcctcatgatacatgggtggccagggtctgtgcgagag
 K  D  V  E  V  I  P  L  L  M  I  H  G  W  P  G  S  V  R  E   160
ttttacgaagcgatccctccgctcacgcgccagacaccaggatacaacttcgtctttgag
 F  Y  E  A  I  P  P  L  T  R  Q  T  P  G  Y  N  F  V  F  E   180
ctgattatgcccagcatacctggctacggtttctctgatcctgcagcaagacccggcctt
 L  I  M  P  S  I  P  G  Y  G  F  S  D  P  A  A  R  P  G  L   200
ggattacccgaagtgagtgtgatcttcaagaacctgatgaacaggcttggatacaagaag
 G  L  P  E  V  S  V  I  F  K  N  L  M  N  R  L  G  Y  K  K   220
ttctatgtgcaaggaggcgattggggcgcagccatcgtgtctaccatgtctaccttattc
 F  Y  V  Q  G  G  D  W  G  A  A  I  V  S  T  M  S  T  L  F   240
cctgaggacattttgggatctcattccaatatgatggtcactcagaacacctgtgcaatg
 P  E  D  I  L  G  S  H  S  N  M  M  V  T  Q  N  T  C  A  M   260
ctgaggtggttcctgggttcgttcttcccttcactggtagttgaagaccatcttgcggat
 L  R  W  F  L  G  S  F  F  P  S  L  V  V  E  D  H  L  A  D   280
agactgtaccctctgtccaaaatgtttgctcattttatggaagagtttggttacatgcat
 R  L  Y  P  L  S  K  M  F  A  H  F  M  E  E  F  G  Y  M  H   300
attcaagctactaaacctgataccgttggcgttcctctcaacgactcccctgccggtcta
 I  Q  A  T  K  P  D  T  V  G  V  P  L  N  D  S  P  A  G  L   320
ctcgcctacatcctggagaagttctccacctggaccaagaacgagtacaagcacaaacca
 L  A  Y  I  L  E  K  F  S  T  W  T  K  N  E  Y  K  H  K  P   340
gacggtggtctcggctccaggttcacgaaagaccagctcatcgacaacctcatgatctac
 D  G  G  L  G  S  R  F  T  K  D  Q  L  I  D  N  L  M  I  Y   360
tggtctactagttctattactacatctatgagattctatgctgagaacatgggagataga
 W  S  T  S  S  I  T  T  S  M  R  F  Y  A  E  N  M  G  D  R   380
gttaggtctcttgcattagatcaaatcaccacaccagtgccatcatgggctctccaggcg
 V  R  S  L  A  L  D  Q  I  T  T  P  V  P  S  W  A  L  Q  A   400
aaagaagagctattctaccagcctcctagtatcctgaagacgaagttcgtcaacctccta
 K  E  E  L  F  Y  Q  P  P  S  I  L  K  T  K  F  V  N  L  L   420
ggcaacacggtcctggatgatggaggccatttcctggctttcgaactgcctgaggttttg
 G  N  T  V  L  D  D  G  G  H  F  L  A  F  E  L  P  E  V  L   440
tcagctgatgtgttcaaggcaatcaaagtattcagagagtggcatgacaagaataagaaa
 S  A  D  V  F  K  A  I  K  V  F  R  E  W  H  D  K  N  K  K   460
actgaactgtgatggggttgttattaaatgtttttttatagtatttttttagaaaaaaaaaa
 T  E  L  *                                                    463
aaaaaaaaaaaaaaaaaaa
```

Fig. 2. Nucleotide (lower case text) and amino acid (upper case text) sequences of *hvmeh1* and Hv-mEH1, respectively. The 5′- and 3′-UTR sequences, and coding sequence of *hvmeh1* were 53, 38, and 1389 nts-long, respectively. Amino acid residues that form the putative catalytic triad (D-227, H-430, and E-403), lid domain (Y-298 and Y-373), and oxyanion hole (HGWP, residues 152–155) are shown in bold text. The asterisk indicates a stop codon (TGA). A putative membrane anchor domain (residues 2–24) that was predicted by SOSUI version 1.11 (Hirokawa et al., 1998) is shown in italic text. Amino acid residue positions are indicated to the right.

2.4.2. Enzyme assays using fluorescent substrates

A series of epoxide containing fluorescent substrates has been developed in our laboratory for use in high throughput assays to screen for inhibitors of EH activity (Jones et al., 2005; Morisseau et al., 2011). The following fluorescent substrates were used in this study: cyano(2-methoxynaphthalen-6-yl)methyl *trans*-2-(3-propyloxiran-2-yl) acetate (**MNHE**); cyano(2-methoxynaphthalen-6-yl)methyl *trans*-(2-(3-phenyloxiran-2-yl))acetate (**MNPE**); cyano-(6-methoxy-naphthalen-2-yl)-methyl *trans*-((3-ethyl-oxiran-2-yl)methyl) carbonate (**MNPEC**); cyano-(6-methoxy-naphthalen-2-yl)-methyl 3,3-dimethyl-oxiranylmethyl carbonate (**MNiPC**); cyano(6-methoxy-naphthalen-2-yl)methyl *trans*-[(3-phenyloxiran-2-yl)methyl] carbonate (**MNPC**); and cyano(6-methoxy-naphthalen-2-yl)methyl oxiran-2-ylmethyl carbonate (**CMNGC**). MNHE, MNPE, MNPEC, MNiPC, and MNPC are previously (Jones et al., 2005) referred to as substrates 2, 3, 4, 6, and 7, respectively. CMNGC is previously (Morisseau et al., 2011) referred to as substrate 11. The specific activity of Hv-mEH1 and MsJHEH for these fluorescent substrates was generally determined as described previously (Jones et al., 2005; Morisseau et al., 2011). The fluorescent assay was routinely performed in 200 μl of 50 mM Tris–HCl buffer, pH 8.0, containing appropriately diluted enzyme, 5 μM substrate (except for CMNGC which was 25 μM), 0.1 mM OTFP (5 min-long preincubation), 1% (v/v) DMSO, and 0.1 mg ml^{-1} BSA in a well of a black 96-well microtiter plate. The reaction was allowed to proceed for 10 min at 30 °C with measurements made at 30 s intervals. Fluorescence was measured in relative fluorescent units (RFU), and absorbance was measured in optical density (OD) with an excitation wavelength of 330 nm and an emission wavelength of 465 nm using a SpectraMax M2 fluorescent plate reader (Molecular Devices). The plate reader settings were as follows: manual gain, 60; integration time, 40 μs; number of flashes, 3. A standard curve was generated to establish the relationship between moles of 6-methoxy-2-naphthaldehyde (Tokyo Kasei Kogyo) and RFU. The resulting calibration curve was used to determine the concentration of the 6-methoxy-2-naphthaldehyde (i.e., fluorescent aldehyde reporter) that was formed in the fluorescent activity assays. Control assays lacking OTFP were also performed to measure the contribution of ester hydrolysis to the formation of the fluorescent aldehyde reporter. All of the assays were performed quadruplicate wells using at least three separate microtiter plates.

2.4.3. Inhibitor assays using fluorescent substrates

The half maximal inhibitory concentration (IC_{50}) of JH-like compounds (ureas, secondary amides, and primary amides) and non-JH-like primary amide compounds against Hv-mEH1, MsJHEH, and hmEH were determined using the fluorescent assays described above. The methods used to synthesize and determine the physical

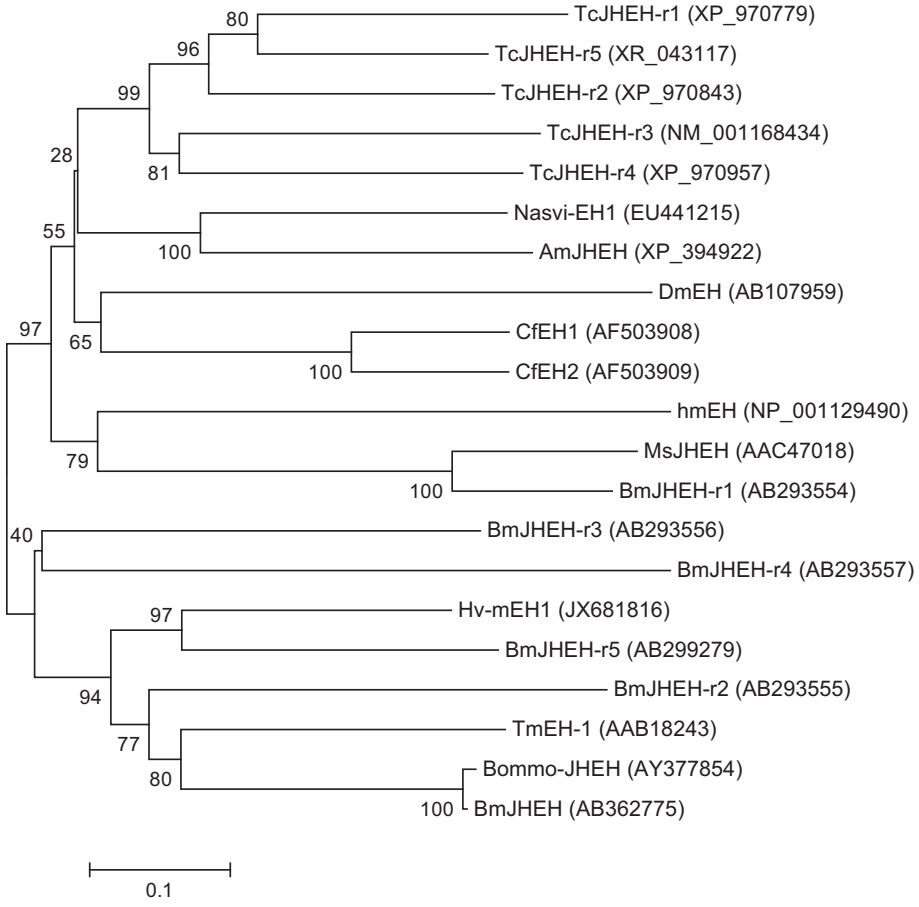

Fig. 3. Phylogenetic relatedness of Hv-mEH1 and JHEH or microsomal EH sequences from five insect orders and Primates. The phylogenetic analysis was performed using MEGA version 5.05 (Tamura et al., 2011). The tree was generated by the Neighbor-Joining method using a ClustalW generated alignment of 21 EH sequences. The percentage of replicate trees in which the sequences clustered together in the bootstrap analysis (1000 replicates) is shown at the branch nodes. The tree is drawn to scale, with branch lengths in the same units as those of the evolutionary distances (computed using the Poisson correction method) used to infer the phylogenetic tree. The GenBank accession number of each sequence is shown within the parenthesis. The insect order and reference of the sequences are as follows. Coleoptera: TcJHEH-r1, -r2, -r3, -r4, and -r5 (Tsubota et al., 2010); Diptera: DmEH (Taniai et al., 2003); Siphonaptera: CfEH1, CfEH2 (Keiser et al., 2002); Hymenoptera: Nasvi-EH1 (Abdel-Latief et al., 2008), AmJHEH (Mackert et al., 2010); Lepidoptera: BmJHEH, BmJHEH-r1, -r2, -r3, -r4, -r5 (Seino et al., 2010), *Bommo*-JHEH (Zhang et al., 2005), MsJHEH (Wojtasek and Prestwich, 1996), TmEH-1 (Harris et al., 1999); Primates: hmEH (Jackson et al., 1987).

characteristics of these compounds are previously described (Morisseau et al., 1999, 2001, 2002; Severson et al., 2002; Morisseau et al., 2008, 2011). Each potential inhibitor was preincubated with the enzyme for 5 min at 30 °C prior to the addition of substrate. Following this preincubation, the substrate (MNPEC for Hv-mEH1 and CMNGC for MsJHEH or hmEH) was added and the reaction was allowed to proceed as described in the previous section. IC_{50} values were determined by regression of at least five datum points, with a minimum of two datum points in the linear region of the curve on either side of the IC_{50} values. The assays were performed in triplicate wells of two independent microtiter plates.

3. Results and discussion

3.1. Cloning and analysis of an EH-encoding cDNA from H. virescens

The full-length, EH-encoding cDNA of *H. virescens* (*hvmeh1*) was identified by 3′- and 5′-RACE and PCR. This approach identified a 1512 nts-long cDNA (GenBank ID: JX681816) that contained an open reading frame of 1389 nts (Fig. 2). The 5′- and 3′-UTR sequences of *hvmeh1* were 53 and 38 nts long, respectively. The deduced protein (Hv-mEH1) of the open reading frame of *hvmeh1* was 463 amino acid residues long (Fig. 2) with a calculated mass of 53,129 Da and predicted pI of 7.23. A 23 amino acid residues-long membrane anchor domain (GFLVKAVLVAALGVTAWFVLKCS) was predicted at the N-terminal (residues 2–24) of Hv-mEH1 by SOSUI version 1.11 (Hirokawa et al., 1998). Amino acid residues that are conserved in the core domain, lid domain, and oxyanion hole motif of biologically active EHs were found in Hv-mEH1 (Fig. 2). The three predicted catalytic residues were D-277, H-430, and E-403. The lid domain residues were Y-298 and Y-373, and oxyanion hole motif was HGWP (residues 152–155). The deduced amino acid sequence of Hv-mEH1 showed approximately 61% identity to *Bommo*-JHEH (Zhang et al., 2005), a silkworm JHEH; 58% identity to TmEH-1 (Harris et al., 1999), a microsomal EH from the lepidopteran *Trichoplusia ni*; and 47% identity to MsJHEH (Wojtasek and Prestwich, 1996), a well-characterized JHEH from the lepidopteran *M. sexta*.

Phylogenetic analysis (Fig. 3) placed Hv-mEH1 in a clade with lepidopteran EHs that generally show low or no detectable JH hydrolytic activity (Harris et al., 1999; Seino et al., 2010). This clade also included *Bommo*-JHEH (Zhang et al., 2005) and BmJHEH (Seino et al., 2010), two EHs that differ by only 5 amino acid residues but show dramatically different activity for JH (Seino et al., 2010). This clade, however, did not include MsJHEH and BmJHEH-r1, two EHs with high JH hydrolytic activity. MsJHEH and BmJHEH-r1 clustered instead in a clade with hmEH (Jackson et al., 1987; Hassett et al., 1994), the major human microsomal EH that is known to be involved in xenobiotic metabolism (Decker et al., 2009).

3.2. Expression and purification of recombinant Hv-mEH1

In order to test if *hvmeh1* encoded a biologically active EH, a recombinant baculovirus, AcHvmEH1, was generated that expressed Hv-mEH1 from *hvmeh1*. AcHvmEH1 produced approximately 38 mg of Hv-mEH1 per liter of insect High Five cells (2×10^6 cells ml^{-1}). Approximately 88% of the total EH activity was found in the microsomal fraction of AcHvmEH1-infected High Five cells at 65 h postinfection. The presence of the majority of the EH activity within the microsomal fraction indicated that the 23 amino acids-long anchor sequence of Hv-mEH1 functioned to retain Hv-mEH1 as a transmembrane protein. Hv-mEH1 represented about 40% of the total protein that was found in the microsomal fraction on the basis of SDS-PAGE analysis (Fig. S1).

3.3. Enzyme activity of Hv-mEH1 with radiolabeled and fluorescent epoxide-containing compounds

Hv-mEH1 metabolized the general EH substrate *c*-SO with a specific activity of 45.8 ± 7.0 nmol min^{-1} mg^{-1} when determined

Table 2
Specific activity of Hv-mEH1, MsJHEH, and hmEH with fluorescent substrates.

Substrate	Structure	Specific activity[a] (nmol min^{-1} mg^{-1})		
		Hv-mEH1	MsJHEH	hmEH
MNHE	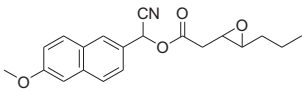	1180 ± 8	38 ± 3	<1.0
MNPE	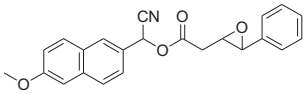	138 ± 9	8.9 ± 0.4	<1.0
MNPEC	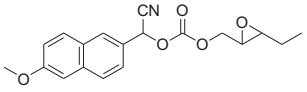	122 ± 11	0.8 ± 0.1	<1.0
MNiPC	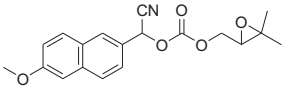	3.7 ± 1.1	1.3 ± 0.5	<1.0
MNPC	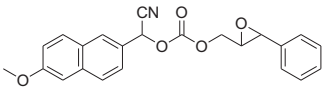	816 ± 140	29 ± 18	<1.0
CMNGC	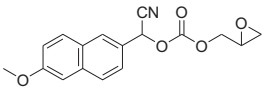	0.03 ± 0.001	3.3 ± 0.2	25 ± 2[b]

[a] The enzyme assays were performed in 50 mM Tris–HCl, pH 8.0, containing 5 μM substrate (25 μM for CMNGC), 100 μM OTFP, 1% (v:v) DMSO, and 0.1 mg ml^{-1} BSA at 30 °C. The results shown are the mean ± standard deviation of at least three separate experiments.
[b] This value is from Morisseau et al. (2011).

in 100 mM sodium phosphate, pH 8.0, at 30 °C. This specific activity was more than 150-fold higher than that of Hv-mEH1 for *t*-SO and *t*-DPPO (Table 1) suggesting a possible preference of Hv-mEH1 for *cis*-epoxides, at least within this series of compounds. In contrast, the specific activities of MsJHEH for *c*-SO and *t*-SO were similar at 3.7 ± 0.5 and 2.1 ± 0.3 nmol min^{-1} mg^{-1}, respectively. In addition, the specific activity of MsJHEH for *t*-DPPO (18.3 ± 4.0 nmol min^{-1} mg^{-1}) was more than 100-fold higher than that of Hv-mEH1 for *t*-DPPO.

We next tested the hypothesis that Hv-mEH1 is an important enzyme in the regulation of JH. The V_{max} of Hv-mEH1 for JH III was 1.7 ± 0.1 nmol of JH III diol formed min^{-1} mg^{-1} when determined in 100 mM sodium phosphate, pH 8.0, at 30 °C. This rate was about 55-fold lower than the V_{max} of authentic, highly purified (i.e., a microsomal preparation subjected to three additional chromatographic separations) MsJHEH (Touhara and Prestwich, 1993), but similar to the specific activity of authentic MsJHEH (Casas et al., 1991) that was prepared by a similar procedure as done in this study. The V_{max} of Hv-mEH1 for JH III was also about 60-fold lower than the specific activity of *Bommo*-JHEH and TcJHEH-r3 (Tsubota et al., 2010), a recombinant coleopteran JHEH. The K_M and k_{cat} values of Hv-mEH1 for JH III were 3200 ± 420 nM and 0.002 s^{-1}, respectively, resulting in a specificity constant (k_{cat}/K_M ratio) of 630 M^{-1} s^{-1}. In comparison, MsJHEH (Touhara and Prestwich, 1993) and *Bommo*-JHEH (Zhang et al., 2005) have K_M values for JH III that are 11- and 6-fold lower, respectively; and k_{cat} values that are 40- and 20-fold faster, respectively. The specificity constants of MsJHEH and *Bommo*-JHEH for JH III (2.9×10^5 M^{-1} s^{-1} and 7.7×10^4 M^{-1} s^{-1}, respectively) are thus 460- and 120-fold higher, respectively, than that of Hv-mEH1. The low specificity constant of Hv-mE1 for JH III argues that Hv-mEH1 may not be the JHEH of *H. virescens*. Should this be the case, *H. virescens* may produce another EH isoform that functions as a JH metabolizing enzyme. This appears to be the case in the lepidopteran *B. mori* in which 6 *jheh*-related genes are found in the genome but apparently only one of these genes encodes an EH that shows significant hydrolytic activity with JH III (Seino et al., 2010). Similarly, there are 5 *jheh*-related genes in the genome of the coleopteran *Tribolium castaneum* but only one of these genes encodes an EH that shows significant hydrolytic activity with JH III (Tsubota et al., 2010).

In our experiments, JH III was used as a model JH primarily because of its commercial availability. JH III is the most widespread of the JH forms that have been identified from insects, but in lepidopteran insects JH 0, JH I or JH II (or a JH precursor or metabolite) may be the predominant form of JH (see Goodman and Granger, 2005). One would expect that the lower steric hindrance of JH III (relative to JH 0, JH I, and JH III) would result in a higher rate of hydrolysis of JH III relative to these other JHs and thus JH III should be a good "model JH". In agreement with this hypothesis, MsJHEH shows significantly higher specificity (k_{cat}/K_M ratio) for JH III in comparison to JH I or JH II (Touhara and Prestwich, 1993). In the case of MsJHEH, the relatively minor substitution of the R methyl group of JH III (Fig. 1) to an ethyl group in JH II (or two ethyl groups at R and R′ in JH I) results in a dramatic 20-fold (or 25-fold in the case of JH I) drop in the specificity constant of MsJHEH (Touhara and Prestwich, 1993). In contrast to MsJHEH, *Bommo*-JHEH shows a specific activity for JH III that is 3- and 5-fold lower than that for JH I and JH II, respectively, (Zhang et al., 2005) indicating that other factors are important in the turnover of JHs. With Hv-mEH1, we believe that the poor turnover and low selectivity that the enzyme showed toward JH III suggests that JH is not the endogenous substrate.

The ability of Hv-mEH1 to metabolize six fluorescent α-cyanoester or α-cyanocarbonate substrates with various epoxide structures (Table 2) was characterized in comparison to MsJHEH and hmEH. Since the specific activity of Hv-mEH1 for JH III was highest at a slightly basic pH (i.e., pH 8.0 and 9.0) and dropped off dramatically at lower pH (Fig. 4), we screened these fluorescent substrates in 50 mM Tris–HCl buffer at pH 8.0. The specific activity of Hv-mEH1 for these fluorescent substrates was generally more than 10-fold higher than the specific activity shown by MsJHEH or hmEH, except in the case of CMNGC (Table 2). Hv-mEH1 showed more than 100-fold lower specific activity for CMNGC, a substrate with a terminal epoxide, in comparison to substrates with 1,2-disubstituted epoxides. Hv-mEH1 showed the highest specific activity for MNHE, an α-cyanoester with an aliphatic 1,2-disubstituted epoxide. This suggested that 1,2-disubstituted epoxides such as fatty acid epoxides might be endogenous substrates for this enzyme as they are for mammalian soluble EHs such as the human EPHX2. *trans*-Aliphatic epoxides and olefins, which can be converted to the corresponding epoxide by cytochrome P450 monooxygenases, are also common in plants as secondary metabolites with roles in plant defense (Krieger et al., 1971; Mullin, 1988). Since *H. virescens* is a generalist feeder one would expect a high level of activity against such secondary compounds in this species.

3.4. Inhibition of Hv-mEH1

In order to further characterize Hv-mEH1, the fluorescent EH assay was used to screen the potency of JH-like urea, JH-like

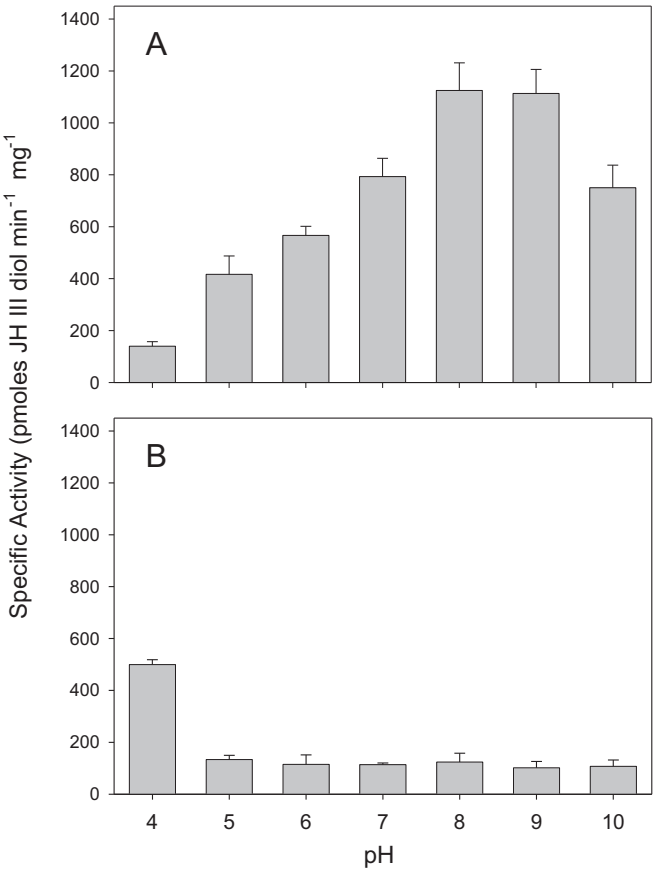

Fig. 4. Effect of pH on the specific activity of Hv-mEH1 for JH III (A) and on non-enzymatic background hydrolysis of JH III (B). The activities were measured in citrate-phosphate (pH 4.0 and 5.0), sodium phosphate (pH 6.0, 7.0, and 8.0) and glycine-sodium hydroxide (pH 9.0 and 10.0) buffer containing 5 μM JH III and 0.1 mg ml^{-1} of BSA. The specific activity values for Hv-mEH1 are corrected for background hydrolysis. The error bars indicate the standard deviation of the mean of at least three independent experiments.

secondary amide, and JH-like primary amide compounds (Table 3) and non-JH-like primary amide compounds (Table 4). A compound was generally considered "JH-like" if it contained an acyclic aliphatic chain of at least 9 carbons. For comparison, the potency of each of these compounds was tested against MsJHEH and hmEH. The JH-like urea compounds were poor inhibitors of Hv-mEH1 but were highly potent (i.e., IC_{50} values less than 1 μM) inhibitors of MsJHEH. In a similar manner, the JH-like secondary amide compounds that showed high (compounds 5 and 6) or moderate (compounds 7 and 8) potency against MsJHEH were poor inhibitors of Hv-mEH1. The JH-like secondary amide compounds with 1,1-dimethyl-ethyl (compound 9) and 1,1-dimethyl-propyl (compound 10) groups attached to the nitrogen were poor inhibitors of both Hv-mEH1 and MsJHEH. In contrast to the JH-like urea and secondary amide compounds, the JH-like primary amide compounds showed high (compounds 11, 12, 14, and 16) or moderate (compound 15)

Table 3
Inhibition of Hv-mEH1, MsJHEH, and hmEH by JH-like urea, secondary amide, and primary amide compounds.

Compound	Structure	IC_{50}[a] (μM)		
		Hv-mEH1	MsJHEH	hmEH
1	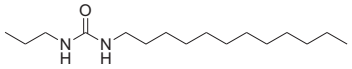	>50	0.4	n.d.
2	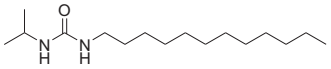	>50	0.5	n.d.
3	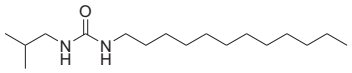	>50	0.3	n.d.
4	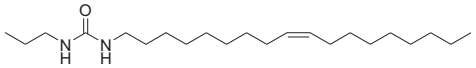	18	0.1	n.d.
5	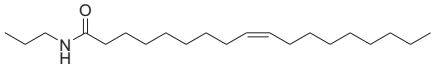	8.1	<0.1	n.d.
6	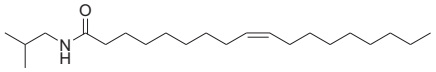	>50	<0.1	n.d.
7	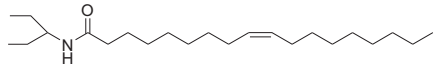	>50	1.9	n.d.
8	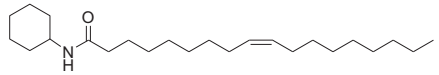	>50	1.7	n.d.
9	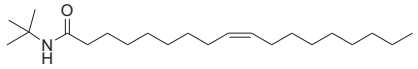	>50	>50	n.d.
10	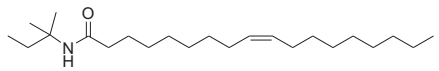	>50	>50	n.d.
11	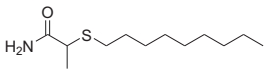	0.1	>50	5.8
12	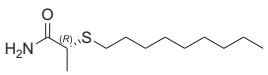	0.6	>50	>50
13	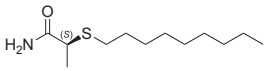	22.5	>50	>50
14	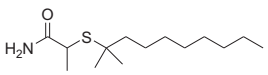	0.3	>50	11.9
15	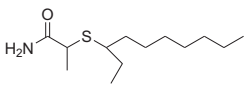	1.7	>50	5.2
16	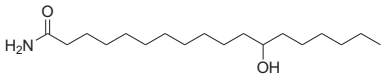	0.2	29.2	>50
17	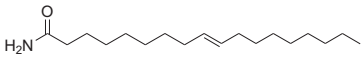	11.1	>50	>50

[a] The enzyme assays were performed in 100 mM Tris–HCl, pH 8.0, containing inhibitor, substrate (5 μM MNPEC for Hv-mEH1 or 25 μM CMNGC for MsJHEH and hmEH), 1% (v:v) DMSO, and 0.1 mg ml^{-1} BSA at 30 °C. The *R/S* configuration of a stereocenter, if known, is indicated by (*R*) and (*S*). The ">50" indicates that less than 50% inhibition was found following incubation with 50 μM of the compound. The "n.d." indicates not determined.

Table 4
Inhibition of Hv-mEH1, MsJHEH, and hmEH by non-JH-like primary amide compounds.

Compound	Structure	IC_{50}[a] (μM)		
		Hv-mEH1	MsJHEH	hmEH
18	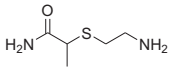	>50	>50	>50
19	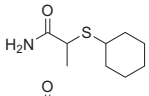	13.7	>50	>50
20	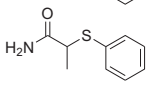	>50	>50	>50
21	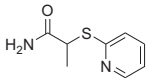	>50	>50	>50
22	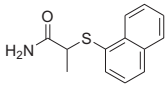	12.0	42.8	43.2
23	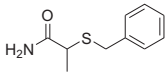	18.9	>50	>50
24	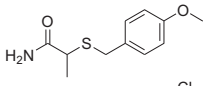	14.9	>50	>50
25	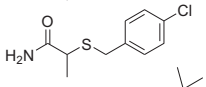	6.3	42.2	>50
26	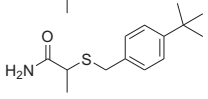	0.8	0.9	>50
27	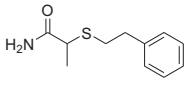	2.5	>50	>50
28	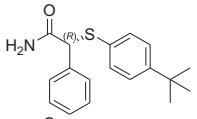	0.1	>50	0.5
29	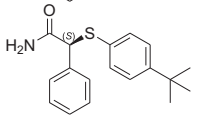	0.3	>50	0.5
30	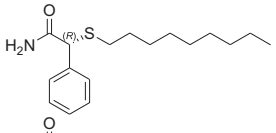	12.8	>50	>50
31	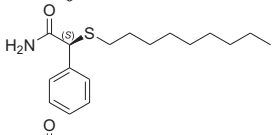	18.2	>50	>50
32	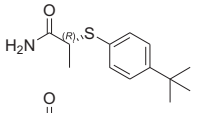	>50	>50	>50
33	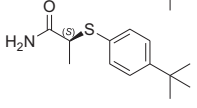	1.5	>50	13.2

[a] The enzyme assays were performed in 100 mM Tris–HCl, pH 8.0, containing inhibitor, substrate (5 μM MNPEC for Hv-mEH1 or 25 μM CMNGC for MsJHEH and hmEH), 1% (v:v) DMSO, and 0.1 mg ml^{-1} BSA at 30 °C. The *R/S* configuration of a stereocenter, if known, is indicated by (*R*) and (*S*). The ">50" indicates that less than 50% inhibition was found following incubation with 50 μM of the compound.

inhibition of Hv-mEH1. On the other hand, the JH-like primary amide compounds were poor inhibitors of both MsJHEH and hmEH.

The non-JH-like primary amide compounds were generally poor inhibitors of Hv-mEH1 (Table 4). The exceptions were compounds 26, 28 and 29, which showed IC_{50}s below 1 μM. The non-JH-like primary amide compounds were also generally poor inhibitors of both MsJHEH and hmEH. The exceptions were again compound 26 for MsJHEH and compounds 28 and 29 for hmEH. There appeared to be no enantiomer selectivity in terms of the potency of compounds 28 and 29, and compounds 30 and 31. However, the *S* enantiomer of compounds 32 and 33, and *R* enantiomer of compounds 12 and 13 appeared to be more potent against Hv-mEH1 than the corresponding *R* and *S* isomers (i.e., compounds 32 and 13, respectively). In summary, the inhibition profiles of Hv-mHE1 and MsJHEH were unique, whereas the inhibition profiles of MsJHEH and hmEH were generally similar. These findings were consistent with the phylogenetic analysis that placed Hv-mEH1 in a clade that was different from the clade formed by MsJHEH, BmJHEH-r1, and hmEH (Fig. 3). In addition, JH-like urea compounds which are generally good inhibitors of MsJHEH (Severson et al., 2002; Garriga and Caballero, 2011) were poor inhibitors of Hv-mEH1 (Table 3). The JH-like secondary amide compounds also followed this trend with the highly potent MsJHEH inhibitors showing significantly lower potency against Hv-mEH1 (Table 3). However, the reverse was often found with the JH-like primary amide compounds, which commonly showed higher potency against Hv-mEH1 in comparison to MsJHEH or hmEH (Table 3).

4. Conclusions

In this study, we obtained a full-length cDNA from *H. virescens* that encodes an epoxide hydrolase. Comparative analysis of the primary sequence of this epoxide hydrolase, Hv-mEH1, suggested that it encodes a JHEH. Hv-mEH1, however, showed slow turnover and high K_M for JH III suggesting that it will function poorly as a JH metabolic enzyme under the physiological conditions of low nanomolar concentrations of JH. We conclude that Hv-mEH1, although capable of metabolizing JH III, is not important in the metabolism of JH in the caterpillar. The very high catalytic activity of this enzyme with some of our model substrates suggests that Hv-mEH1 may have a role in the hydration of xenobiotics in the diet or an endogenous epoxide that is yet to be identified. Hopefully, the powerful inhibitors described here will help expand our understanding of the physiological role of Hv-mEH1 in the caterpillar.

Acknowledgments

This work was funded by grants from the USDA (#2007-35607-17830) and NIEHS (#R01 ES002710 and #P42 ES04699). We thank Aman I. Samra and Hongwei Yao for help with the cloning experiments, and Paul Jones for the synthesis of some of the fluorescent substrates.

Appendix A. Supplementary data

Supplementary data related to this article can be found at http://dx.doi.org/10.1016/j.ibmb.2012.12.002.

References

Abdel-Aal, Y.A.I., Hammock, B.D., 1985. 3-Octylthio-1,1,1-trifluoro-2-propanone, a high affinity and slow binding inhibitor of juvenile hormone esterase from *Trichoplusia ni* (Hubner). Insect Biochem. 15, 111–122.

Abdel-Latief, M., Garbe, L.A., Koch, M., Ruther, J., 2008. An epoxide hydrolase involved in the biosynthesis of an insect sex attractant and its use to localize the production site. Proc. Natl. Acad. Sci. USA 105, 8914–8919.

Borhan, B., Mebrahtu, T., Nazarian, S., Kurth, M.J., Hammock, B.D., 1995. Improved radiolabeled substrates for soluble epoxide hydrolase. Anal. Biochem. 231, 188–200.
Casas, J., Harshman, L.G., Hammock, B.D., 1991. Epoxide hydrolase activity on juvenile hormone in *Manduca sexta*. Insect Biochem. 21, 17–26.
Debernard, S., Morisseau, C., Severson, T.F., Feng, L., Wojtasek, H., Prestwich, G.D., Hammock, B.D., 1998. Expression and characterization of the recombinant juvenile hormone epoxide hydrolase (JHEH) from *Manduca sexta*. Insect Biochem. Mol. Biol. 28, 409–419.
Decker, M., Arand, M., Cronin, A., 2009. Mammalian epoxide hydrolases in xenobiotic metabolism and signalling. Arch. Toxicol. 83, 297–318.
Dietze, E.C., Kuwano, E., Hammock, B.D., 1994. Spectrophotometric substrates for cytosolic epoxide hydrolase. Anal. Biochem. 216, 176–187.
Fitt, G.P., 1989. The ecology of *Heliothis* species in relation to agroecosystems. Annu. Rev. Entomol. 34, 17–52.
Garriga, M., Caballero, J., 2011. Insights into the structure of urea-like compounds as inhibitors of the juvenile hormone epoxide hydrolase (JHEH) of the tobacco hornworm *Manduca sexta*: analysis of the binding modes and structure-activity relationships of the inhibitors by docking and CoMFA calculations. Chemosphere 82, 1604–1613.
Gill, S.S., Ota, K., Hammock, B.D., 1983. Radiometric assays for mammalian epoxide hydrolases and glutathione *S*-transferase. Anal. Biochem. 131, 273–282.
Goodman, W.G., Granger, N.A., 2005. The juvenile hormones. In: Gilbert, L.I., Iatrou, K., Gill, S.S. (Eds.), Comprehensive Molecular Insect Science, vol. 3. Elsevier, Oxford, pp. 319–408.
Hammock, B.D., Sparks, T.C., 1977. A rapid assay for insect juvenile hormone esterase activity. Anal. Biochem. 82, 573–579.
Harris, S.V., Thompson, D.M., Linderman, R.J., Tomalski, M.D., Roe, R.M., 1999. Cloning and expression of a novel juvenile hormone-metabolizing epoxide hydrolase during larval-pupal metamorphosis of the cabbage looper, *Trichoplusia ni*. Insect Mol. Biol. 8, 85–96.
Hassett, C., Robinson, K.B., Beck, N.B., Omiecinski, C.J., 1994. The human microsomal epoxide hydrolase gene (EPHX1): complete nucleotide sequence and structural characterization. Genomics 23, 433–442.
Hirokawa, T., Boon-Chieng, S., Mitaku, S., 1998. SOSUI: classification and secondary structure prediction system for membrane proteins. Bioinformatics 14, 378–379.
Jackson, M.R., Craft, J.A., Burchell, B., 1987. Nucleotide and deduced amino acid sequence of human liver microsomal epoxide hydrolase. Nucleic Acids Res. 15, 7188.
Jones, P.D., Wolf, N.M., Morisseau, C., Whetstone, P., Hock, B., Hammock, B.D., 2005. Fluorescent substrates for soluble epoxide hydrolase and application to inhibition studies. Anal. Biochem. 343, 66–75.
Kamita, S.G., Hammock, B.D., 2010. Juvenile hormone esterase: biochemistry and structure. J. Pestic. Sci. 35, 265–274.
Keiser, K.C.L., Brandt, K.S., Silver, G.M., Wisnewski, N., 2002. Cloning, partial purification and in vivo developmental profile of expression of the juvenile hormone epoxide hydrolase of *Ctenocephalides felis*. Arch. Insect Biochem. Physiol. 50, 191–206.
Kotaki, T., Shinada, T., Kaihara, K., Ohfune, Y., Numata, H., 2009. Structure determination of a new juvenile hormone from a heteropteran insect. Org. Lett. 11, 5234–5237.
Krieger, R.I., Feeny, P.P., Wilkinson, C.F., 1971. Detoxication enzymes in the guts of caterpillars: an evolutionary answer to plant defenses? Science 172, 579–581.
Mackert, A., Hartfelder, K., Bitondi, M.M.G., Simoes, Z.L.P., 2010. The juvenile hormone (JH) epoxide hydrolase gene in the honey bee (*Apis mellifera*) genome encodes a protein which has negligible participation in JH degradation. J. Insect Physiol. 56, 1139–1146.
Merrington, C.L., King, L.A., Posse, R.D., 1999. Baculovirus expression systems. In: Higgins, S.J., Hames, B.D. (Eds.), Protein Expression: A Practical Approach. Oxford University Press, pp. 101–127.
Mitter, C., Poole, R.W., Matthews, M., 1993. Biosystematics of the Heliothinae (Lepidoptera, Noctuidae). Annu. Rev. Entomol. 38, 207–225.
Morisseau, C., Bernay, M., Escaich, A., Sanborn, J.R., Lango, J., Hammock, B.D., 2011. Development of fluorescent substrates for microsomal epoxide hydrolase and application to inhibition studies. Anal. Biochem. 414, 154–162.
Morisseau, C., Goodrow, M.H., Dowdy, D.L., Zheng, J., Greene, J.F., Sanborn, J.R., Hammock, B.D., 1999. Potent urea and carbamate inhibitors of soluble epoxide hydrolases. Proc. Natl. Acad. Sci. USA 96, 8849–8854.
Morisseau, C., Goodrow, M.H., Newman, J.W., Wheelock, C.E., Dowdy, D.L., Hammock, B.D., 2002. Structural refinement of inhibitors of urea-based soluble epoxide hydrolases. Biochem. Pharmacol. 63, 1599–1608.
Morisseau, C., Hammock, B.D., 2005. Epoxide hydrolases: mechanisms, inhibitor designs, and biological roles. Annu. Rev. Pharmacol. Toxicol. 45, 311–333.
Morisseau, C., Hammock, B.D., 2008. Gerry Brooks and epoxide hydrolases: four decades to a pharmaceutical. Pest Manag. Sci. 64, 594–609.
Morisseau, C., Newman, J.W., Dowdy, D.L., Goodrow, M.H., Hammock, B.D., 2001. Inhibition of microsomal epoxide hydrolases by ureas, amides, and amines. Chem. Res. Toxicol. 14, 409–415.
Morisseau, C., Newman, J.W., Wheelock, C.E., Hill, T., Morin, D., Buckpitt, A.R., Hammock, B.D., 2008. Development of metabolically stable inhibitors of mammalian microsomal epoxide hydrolase. Chem. Res. Toxicol. 21, 951–957.
Mullin, C.A., 1988. Adaptive relationships of epoxide hydrolase in herbivorous arthropods. J. Chem. Ecol. 14, 1867–1888.
Rasband, W.S., 2006. ImageJ. U. S. National Institutes of Health, Bethesda, Maryland. http://rsb.info.nih.gov/ij/.
Riddiford, L.M., 2008. Juvenile hormone action: a 2007 perspective. J. Insect Physiol. 54, 895–901.
Seino, A., Ogura, T., Tsubota, T., Shimomura, M., Nakakura, T., Tan, A., Mita, K., Shinoda, T., Nakagawa, Y., Shiotsuki, T., 2010. Characterization of juvenile hormone epoxide hydrolase and related genes in the larval development of the silkworm *Bombyx mori*. Insect. Mol. Biol. 74, 1421–1429.
Severson, T.F., Goodrow, M.H., Morisseau, C., Dowdy, D.L., Hammock, B.D., 2002. Urea and amide-based inhibitors of the juvenile hormone epoxide hydrolase of the tobacco hornworm (*Manduca sexta*: Sphingidae). Insect Biochem. Mol. Biol. 32, 1741–1756.
Shan, G.M., Hammock, B.D., 2001. Development of sensitive esterase assays based on alpha-cyano-containing esters. Anal. Biochem. 299, 54–62.
Tamura, K., Peterson, D., Peterson, N., Stecher, G., Nei, M., Kumar, S., 2011. MEGA5: molecular evolutionary genetics analysis using maximum likelihood, evolutionary distance, and maximum parsimony methods. Mol. Biol. Evol. 28, 2731–2739.
Taniai, K., Inceoglu, A.B., Yukuhiro, K., Hammock, B.D., 2003. Characterization and cDNA cloning of a clofibrate-inducible microsomal epoxide hydrolase in *Drosophila melanogaster*. Eur. J. Biochem. 270, 4696–4705.
Touhara, K., Prestwich, G.D., 1993. Juvenile hormone epoxide hydrolase - photoaffinity-labeling, purification, and characterization from tobacco hornworm eggs. J. Biol. Chem. 268, 19604–19609.
Tsubota, T., Nakakura, T., Shiotsuki, T., 2010. Molecular characterization and enzymatic analysis of juvenile hormone epoxide hydrolase genes in the red flour beetle *Tribolium castaneum*. Insect Mol. Biol. 19, 399–408.
Weyer, U., Knight, S., Possee, R.D., 1990. Analysis of very late gene expression by *Autographa californica* nuclear polyhedrosis virus and the further development of multiple expression vectors. J. Gen. Virol. 71, 1525–1534.
Wheelock, C.E., Wheelock, A.M., Zhang, R., Stok, J.E., Morisseau, C., Le Valley, S.E., Green, C.E., Hammock, B.D., 2003. Evaluation of alpha-cyanoesters as fluorescent substrates for examining interindividual variation in general and pyrethroid-selective esterases in human liver microsomes. Anal. Biochem. 315, 208–222.
Wixtrom, R.N., Hammock, B.D., 1985. Membrane-bound and soluble fraction epoxide hydrolases: methodological aspects. In: Zakim, D., Vessey, D.A. (Eds.), Biochemical Pharmacology and Toxicology, vol. 1. John Wiley and Sons, New York, pp. 1–93.
Wojtasek, H., Prestwich, G.D., 1996. An insect juvenile hormone-specific epoxide hydrolase is related to vertebrate microsomal epoxide hydrolases. Biochem. Biophys. Res. Commun. 220, 323–329.
Yamada, T., Morisseau, C., Maxwell, J.E., Argiriadi, M.A., Christianson, D.W., Hammock, B.D., 2000. Biochemical evidence for the involvement of tyrosine in epoxide activation during the catalytic cycle of epoxide hydrolase. J. Biol. Chem. 275, 23082–23088.
Zhang, Q.R., Xu, W.H., Chen, F.S., Li, S., 2005. Molecular and biochemical characterization of juvenile hormone epoxide hydrolase from the silkworm, *Bombyx mori*. Insect. Biochem. Mol. Biol. 35, 153–164.